Listeria monocytogenes CadC regulates cadmium efflux and fine-tunes lipoprotein localization to escape the host immune response and promote infection

Rita Pombinho[1,2,3,#], Ana Camejo[1,2,3,#], Ana Vieira[1,2], Olga Reis[1,2,3], Filipe Carvalho[1,2,3], Maria Teresa Almeida[1,2,3], Jorge Campos Pinheiro[1,2,3], Sandra Sousa[1,2], Didier Cabanes[1,2,*]

[1] Instituto de Investigação e Inovação em Saúde – i3S, Universidade do Porto, Porto, Portugal

[2] Group of Molecular Microbiology, Instituto de Biologia Molecular e Celular - IBMC, Porto, Portugal

[3] Instituto de Ciências Biomédicas Abel Salazar, Universidade do Porto, Porto, Portugal

[#] Equally contributed to this work

[*] Corresponding author: didier@ibmc.up.pt

Running title: *Listeria* CadC fine-tunes lipoprotein release

Footnote

Conflict of interest: No conflict of interest

Funding information:

This work was supported for the D.C. lab by national funds through FCT - Fundação para a Ciência e a Tecnologia/MEC - Ministério da Educação e Ciência and co-funded by FEDER funds within the partnership agreement PT2020 related with the research unit number 4293, and within the research project Infect-ERA/0001/2013 PROANTILIS. A.C., R.P., O.R., F.C., MT.A. and J.C.P. were supported by doctoral fellowships from FCT (SFRH/BD/29314/2006, SFRH/BD/89542/2012, SFRH/BD/28185/2006, SFRH/BD/61825/2009, SFRH/BD/43352/2008 and SFRH/BD/86871/2012) and SS was supported by FCT Investigator program (COMPETE, POPH, and FCT).

Corresponding author:

Didier cabanes

IBMC - Instituto de Biologia Molecular e Celular, Group of Molecular Microbiology

Rua do Campo Rua Alfredo Allen, 208

4200-135 Porto

Portugal

Tel: +351 220 408 800 Ext. 6099

e-mail: didier@ibmc.up.pt

ABSTRACT

Listeria monocytogenes (*Lm*) is a major intracellular human foodborne bacterial pathogen. We previously revealed *Lm-cadC* as highly expressed during mouse infection. Here we show that *Lm*-CadC is a sequence-specific, DNA-binding and cadmium-dependent regulator of CadA, an efflux pump conferring cadmium resistance. CadC, but not CadA, is required for *Lm* infection *in vivo*. Interestingly, CadC also directly represses *lspB*, a gene encoding a lipoprotein signal peptidase whose expression appears detrimental for infection. *lspB* overexpression promotes the release of the LpeA lipoprotein to the extracellular medium, inducing TNF-α and IL-6 expression, thus impairing *Lm* survival in macrophages. We propose that *Lm* uses CadC to repress *lspB* expression during infection to avoid LpeA exposure to the host immune system, diminishing inflammatory cytokine expression and promoting intramacrophage survival and virulence. CadC appears as the first metal efflux pump regulator repurposed during infection to fine-tune lipoprotein processing and host responses.

Word count: 145

Keywords: *Listeria*/virulence factor; CadAC; Gram-positive; host-response; pathogen

BACKGROUND

Despite their toxicity at high concentration, some heavy metals are required as cofactors for enzymatic reactions or as structural components of bacterial proteins. Therefore, their intracellular concentration needs to be finely tuned to maintain metal homeostasis. Efflux pumps are usually substrate-specific and control intracellular metal concentrations conferring heavy metal resistance [1, 2]. In its ionized form cadmium is toxic for many organisms, including bacteria. Erosion, forest fires and volcanic eruptions are natural sources of cadmium which is dispersed into air, water, soils and foodstuffs. Cadmium resistance systems are commonly composed by a metal-responsive transcriptional repressor (CadC) belonging to the ArsR-SmtB family [3-5], and a P1-type ATPase (CadA) that extrudes heavy metals from the cell [6].

Listeria monocytogenes is a major intracellular foodborne bacterial pathogen causing listeriosis, a systemic infection in humans [7]. Among zoonotic diseases under EU-surveillance, listeriosis is the most severe with 99.1% of the cases hospitalized and a case fatality rate of 15.6% [8]. Listeriosis is clinically characterized by septicemia and dissemination to the nervous system and fetal-placental unit [9]. As a foodborne pathogen, *L. monocytogenes* has the capacity to colonize various niches, ranging from inert and organic matrixes to the intestinal lumen where it competes with resident microbiota, translocates across the epithelium, multiplies in phagocytic and non-phagocytic cells, disseminates *via* the blood and evades the immune response [7]. A functional CadAC system was previously identified in *L. monocytogenes* Lm74 on the Tn5422 transposable element harbored by the pLm74 plasmid [10, 11], and was shown to be induced by and to confer resistance to cadmium [11]. We previously showed that, in *L. monocytogenes* EGDe (*Lm*), *cadC* is highly expressed during infection and required for *Lm* virulence [12].

Here we characterize the *Lm* cadmium resistance system and discover an unexpected role of CadC in bacterial pathogenicity.

METHODS

Bacteria and cells

Lm (ATCC-BAA-679) [13] were grown in BHI (BD-Difco) at 37ºC with erythromycin (5 μg/ml), chloramphenicol (7 μg/ml). *Escherichia coli* were grown in LB at 37ºC with ampicillin (100 μg/ml), erythromycin (300 μg/ml), kanamycin (30 μg/ml). RAW-264.7 (ATCC-TIB-71) were cultured in DMEM 10% FBS (Lonza), BMDM in DMEM 10 mM HEPES, 10% FBS and 10% L929-conditioned medium at 37ºC, 5% CO_2.

Deletions (Δ*cadA*, Δ*cadC,* Δ*cadAC,* Δ*lspB,* Δ*cadC*Δ*lspB*), insertion (Δ*lpeA*) and complementation (Δ*cadC*+*cadC*) were performed as described [14, 15]. Overexpression (WT+*lspB)* was performed using pMK4-vector [16] carrying the strong constitutive Pprot-promoter [17, 18]. Primers are listed Tab.S1. Constructs were confirmed by sequencing.

Toxicity assays

Cadmium challenge: 1/100-diluted overnight cultures were challenged after 210 min with 384 μM $CdCl_2$. Growth (OD_{600}) was measured every 45 min. Disk diffusion assays: plated bacterial lawns were overlaid with 6-mm paper-disk soaked with 10 μl of metal salt solution (100 mM). Growth inhibition zone diameter was measured after overnight incubation at 37ºC. MICs: 96-wells microtiter plates containing BHI/metal-salt solutions (100/100 μl) were inoculated with 1 μl of overnight cultures. Growth was assessed (OD_{600}) after 24h incubation at 37ºC.

Inductively coupled plasma mass spectrometry (ICP-MS)

Bacterial cultures (OD_{600}=0.6) were supplemented with 384 μM $CdCl_2$ 15 min, centrifuged, PBS-washed and lyophilized. Dried samples were digested with HNO_3, suspended in 4N HNO_3, diluted in water and analyzed by ICP-MS.

Proteins

cadC was cloned into pET28b, sequenced, and transformed in *E. coli* BL21(DE3). CadC-His_6 production was induced with 0.1mM IPTG at 37ºC 3h. Cells were re-suspended, sonicated, cleared by centrifugation and soluble fraction purified by Ni-NTA-agarose chromatography (QIAGEN).

Lipoproteins were recovered by Triton X-114 phase-partitioning method [19] and culture supernatant proteins by TCA precipitation [20].

SDS-PAGE protein bands were excised, reduced with DTT, alkylated with iodoacetamide and in-gel digested with trypsin. Peptide identification was performed by MALDI TOF/TOF mass spectrometry [21].

Electrophoretic mobility shift assays (EMSAs)

CadC-DNA binding assays were performed in 50 mM Tris-HCl pH7.4, 6 mM $MgCl_2$, 100 mM NaCl, 50 mM KCl, 100 ng DNA and purified CadC/GFP. After 20 min at RT samples were resolved in 6% polyacrylamide gel and visualized by DNA staining.

ChIP-qPCR

Chromatin immunoprecipitation (ChIP) were performed as described [22] using anti-CadC polyclonal rabbit serum generated through CadC-His_6 as described [15]. 1-10 ng of ChIP Purified DNA (NZYGelpure) was analyzed by qPCR.

Macrophage infection

Bone marrow cells were collected from C57BL/6 mouse femurs and differentiated 10 days. *Lm* (OD_{600}=0.8) were added to BMDM or RAW at MOI 10 for 20/30 min. Macrophages were treated 10 min/4h30 with 20 µg/ml gentamicin, washed, lysed (0.1% Triton X-100) and intracellular bacteria enumerated by plating.

Transmission electron microscopy

Lm (OD_{600}=0.8) were fixed 1h at RT (4% paraformaldehyde, 2.5% glutaraldehyde, 0.1 M sodium-cacodylate, pH7.2), stained 2h with 1% osmium tetroxide and compacted in 30% BSA. Bacterial pellets were fixed overnight in 1% glutaraldehyde, dehydrated in ethanol and embedded in Epon-812. Ultrathin sections (40-50 nm) were placed on 400-mesh copper grids and visualized (Jeol JEM-1400).

RNA techniques

RNAs were extracted from *Lm* (OD_{600}=0.8) and RAW (5h p.i.), treated (TURBO-DNA-free, Ambion), quality-checked (Experion, Bio-Rad-Laboratories), reverse-transcribed (iScript, Bio-Rad-Laboratories) and analyzed by

qRT-PCR as described [12]. Gene expression data were analyzed by comparative Ct method [23], normalized to relative reference gene expression (*Lm* 16S rRNA or *Mus musculus hprt1*).

Mouse infections

Intravenous and oral inoculations were performed as described [24] (n=5). Animal procedures were in agreement with European Commission (directive 2010/63/EU) and Portuguese (Decreto-Lei 113/2013) guidelines, approved by IBMC Ethics Committee and Direcção Geral Veterinária (license PTDC/SAU-MIC/111581/2009).

ELISA

Cytokine levels released into infected RAW supernatant were measured using murine ELISA kit (eBioscience).

Statistics

Statistics were performed with Prism (GraphPad), using unpaired two-tailed Student's *t*-test to compare means of two groups, and one-way ANOVA with Tukey's post-hoc test for pairwise comparison of means from more than two groups, or with Dunnett's post-hoc test for comparison of means relative to the mean of a control group.

RESULTS

L. monocytogenes chromosomally encodes a cadmium efflux system expressed in the presence of cadmium and independently of PrfA

Lm-cadAC encode proteins with high level of identity to CadAC cadmium efflux systems from several species (Fig.1AB, S1A). *Lm*-CadC displays classical DNA-binding helix-turn-helix motif and type-1 metal-binding site composed of four critical cysteines [25] (Fig.1A). The predicted *Lm*-CadC structure is close to *Staphylococcus aureus* (*Sa*) CadC (Fig.S1B). However, *Lm*-CadC lacks the type-2 metal-binding site present in *Sa*-CadC but dispensable for metal binding [26] (Fig.1A). *Lm*-CadA exhibits metal-binding domain and motifs conserved in P1-type ATPases, and is predicted to be a membrane protein with 8 transmembrane domains (Fig.S1C) [27]. Whereas harbored by plasmids in different *Listeria* strains [10, 11, 28], *cadA and cadC* are located on the *Lm* chromosome. *Lm-cadA* is found downstream of *cadC*, with an oppositely oriented gene in between (*lspB*) encoding a putative lipoprotein signal peptidase type-II [29, 30] (Fig.1B). *cadA-lspB-cadC* are flanked by an

integrase-encoding gene (*lmo1097*) and 12 Tn916-like genes (*lmo1103-lmo1114*). The average GC content percentage (32%) of the *lmo1097-lmo1102* locus is notably lower than that of surrounding regions (39-43%) (Fig.1B).

We first analyzed whether *cadA, lspB and cadC* are transcribed from a single promoter. Whereas in presence of cadmium (Cd), independent transcripts were detected for the three genes, no co-transcript was observed (Fig.1C), indicating that in the conditions tested there is no *cadA-lspB-cadC* co-transcription.

PrfA controls the expression of major *Lm* virulence genes [31, 32]. We found a palindromic sequence TTAACAgaTTTCAA, bearing two mismatches with the consensus PrfA-box (TTAACAttTGTTAA), 661-bp upstream *cadC* start codon. PrfA-dependent *cadC* transcription was assessed on wild type (WT) and Δ*prfA* strains grown in BHI or glycerol-supplemented minimal medium (MM), in presence of Cd. PrfA is fully active in MM [33]. Levels of *cadC* transcripts were similar in both strains under both conditions (Fig.1D), demonstrating that PrfA does not control *cadC* expression.

Thus, *Lm* encodes a chromosomal putative Cd efflux system whose expression is Cd-dependent and PrfA-independent.

CadA is a functional cadmium efflux pump required for *Lm* resistance to cadmium

Growth rates of single (Δ*cadA,* Δ*cadC*) and double (Δ*cadAC*) deletion mutants were comparable to that of WT strain (Fig.2A), indicating that none of the Cad proteins is essential for viability/growth in rich medium. Addition of Cd to mid-exponential cultures induced a slight decrease on WT and Δ*cadC* growth, whereas it notably impaired the growth of Δ*cadA* and Δ*cadAC*, revealing the CadA role in *Lm* resistance to Cd. While growth inhibition zone registered when *Lm* lawns were grown on BHI plates overlaid with disks saturated with $CdCl_2$ was equivalent in WT and Δ*cadC*, Δ*cadA* displayed increased Cd susceptibility (Fig.2B), confirming the role of CadA in Cd resistance and demonstrating that CadC is not required for Cd resistance. Similar areas of growth inhibition were observed with disks saturated either with $CdCl_2$ or $CdSO_4$ (Fig.2B), showing that Cd is the cause of toxicity. WT and Δ*cadA* showed similar growth inhibition in response to all other metal salts tested (Fig.2B), indicating that

CadA mainly confers resistance to Cd. In agreement, as compared to WT, Δ*cadA* displayed a 10-fold decrease in minimum inhibitory concentration (MIC) of Cd, while it remained unchanged for Zn, Co, Cu and Ni (Fig.2C). We measured intracellular levels of Cd, Zn and Pb in WT and Δ*cadA*. Whereas Zn and Pb levels were equivalent in both strains, Δ*cadA* accumulated nearly 6-fold more intracellular Cd (Fig.2D), demonstrating that CadA is required to maintain homeostatic intracellular Cd concentrations.

These results confirm that *Lm*-CadA is a functional Cd efflux pump required to confer resistance to Cd-induced toxicity.

CadC directly regulates *cadA, cadC* and *lspB* expression in response to cadmium

We assessed the role of CadC and Cd in *cadA, cadC* and *lspB* transcription. In absence of CadC*, cadA* and *lspB* transcript levels were significantly increased, and *cadA*, *cadC* and *lspB* transcripts rose in response to Cd (Fig.3A), showing that CadC actively represses *cadA* and *lspB* transcription, whereas Cd activates *cadA, cadC* and *lspB* expression.

We identified conserved CadC-boxes (Cx) exclusively in the promoter regions of *cadA* (*cadA*-Cx), *cadC* (*cadC*-Cx) and *lspB* (*lspB*-Cx), similar to the well-characterized *Sa*-Cx (Fig.3B). *Lm* CadC was produced, purified (Fig.S2A) and used in EMSAs with DNA-fragments containing each Cx. CadC appeared capable to delay the migration of *cadA*-Cx, *cadC*-Cx and *lspB*-Cx (Fig.3B), but not of a negative control promoter DNA (*inlA*). Similarly, an unrelated protein (GFP) did not delay *cadC-Cx* migration. Thus, direct CadC binding to Cx appears to be sequence- and protein-specific. To confirm that *Lm*-CadC binds to Cx *in vivo*, CadC was immunoprecipitated from *Lm* extracts using an anti-CadC antibody, and co-precipitated DNA was analyzed by qPCR using primers specific for the different Cx (ChIP-qPCR). An enrichment was observed for all Cx tested (Fig.3B), and shown to be specific by normalization to a negative control DNA and to mock-IP, demonstrating the CadC binds specifically to *Lm*-Cx *in vivo.*

EMSAs were also performed with DNA fragments containing wild-type *cadC*-Cx sequence (Cx) or with point (Cx-M1-6) or transversed (Cx-T) mutations (Fig.3C). Whereas CadC altered the migration of native Cx, with the

exception of the M2 substitution (T→G), every other mutation abrogated the mobility shift. The CadC-Cx interaction appears thus highly specific and dependent on the conserved palindromic sequence.

In the presence of increased concentrations of Cd, CadC was released from Cx (Fig.3D). In addition, the Cd concentration necessary to abrogate CadC binding to Cx was ten-fold lower than that required to prevent CadC binding to a DNA fragment containing two Cx (*cadA*-Cx-*lspB*-Cx).

These results demonstrate that, in absence of Cd, CadC represses the expression of *cadAC* by directly binding conserved Cx present in *cadA* and *cadC* promoters. In presence of Cd, CadC cannot bind to or is detached from Cx, allowing CadA expression, thus inducing Cd resistance. The Cd concentration required to prevent CadC binding depends on the number of Cx. The expression of *lspB* is also subjected to Cd-dependent CadC-mediated regulation. However, *lspB* appears needless for Cd resistance (Fig.S2B).

CadC is required for efficient *Lm* infection *in vivo*

We evaluated the role of CadAC during *Lm* infection *in vivo* by determining bacterial loads in liver and spleen of intravenously inoculated mice. 72h post-infection (p.i.), bacterial counts for the WT and Δ*cadA* were similar in both organs (Fig.4A). However, they appeared significantly lower for Δ*cadC* and Δ*cadAC*. Complementation of the Δ*cadC* mutant (Δ*cadC*+*cadC*) restored bacterial loads to WT levels. Oral inoculation confirmed the impaired colonization of mouse organs by the Δ*cadC* and Δ*cadAC* as compared to the WT and Δ*cadA* strains (Fig.4B). CadC thus plays a role in *Lm in vivo* infection, independent of *cadA* expression.

In absence of CadC repression, *lspB* expression is deleterious for *Lm* infection

CadC being overexpressed in mouse organs [12], we postulated that CadC-dependent *lspB* repression would be necessary for efficient *Lm* infection. We constructed Δ*lspB* and Δ*cadC*Δ*lspB* mutants and a *lspB*-overexpressing strain (WT+*lspB*). Analysis of growth rates and *lspB* transcription indicated that neither the absence nor the overexpression of *lspB* have significant impact on *Lm* viability/replication in rich medium (Fig.S2DE). TEM micrographs revealed no difference regarding overall and cell wall morphology of *lspB*-overexpressing strains (Fig.S2F). 72h post mouse intravenous (Fig.4C) or oral (Fig.4D) inoculation, bacterial counts for the WT and Δ*lspB*

were not significantly different, indicating that LspB is not required for *Lm* infection. Interestingly, whereas Δ*cadC* bacteria were attenuated (Fig.4AD), Δ*cadC*Δ*lspB* behaved like the WT (Fig.4CD), suggesting that the Δ*cadC* phenotype is associated to *lspB* expression levels. In agreement, the *lspB*-overexpressing strain appeared significantly attenuated both after intravenous (Fig.4C) or oral (Fig.4D) inoculation.

Increased *lspB* expression, either through the absence of CadC repression or through overexpression, appears thus detrimental for the *Lm* infectious capacity.

LspB controls LpeA extracellular release

LspB has a high identity degree with known signal-peptidase-type-II (SPase-II) from other *Listeria* strains and bacterial species (Fig.5A), in particular with the *S. thermophilus* (*St*) SPase-II (75% identity). LspB harbors the five highly conserved SPase-II domains and the six residues critical for SPase-II activity [34]. Predicted LspB topology shows the presence of four transmembrane domains, suggesting a membrane localization (Fig.S1D). SPases-II were shown to be involved in lipoprotein membrane insertion and release to the extracellular medium [35]. We thus hypothesized that differential *lspB* expression could result in changes in the repertoire of *Lm* surface-exposed and/or released lipoproteins. Whereas no difference was observed in membrane lipoprotein extracts, a band was detected between 25-37 kDa with increased intensity in culture supernatants from *lspB*-overexpressing strains (Δ*cadC,* WT+*lspB*) (Fig.5BC). The protein present in this band was identified by mass spectrometry as the *Lm* lipoprotein LpeA (Lipoprotein promoting entry A) [36] (Tab.S3). LspA was the first SPase-II identified in *Lm* [44]. We analyzed *lspA* expression levels and showed that they were similar in the different strains (Fig.S3A), indicating that increased LpeA levels in culture supernatants from *lspB*-overexpressing strains are unrelated to a differential *lspA* expression.

Thus, *lspB* encodes a secondary *Lm* SPase-II which promotes the release of the LpeA lipoprotein to the extracellular medium.

***lspB* derepression induces expression of inflammatory cytokines limiting intramacrophagic survival**

LpeA was shown to be required for entry into intestinal and hepatic cells [36]. In addition, a LpeA-deficient mutant survives longer in macrophages and is slightly more virulent in mice than WT bacteria [36]. We thus hypothesized that in presence of high LspB levels, more LpeA would be found in the extracellular medium, which would decrease *Lm* survival in macrophages. We analyzed the capacity of *Lm* strains to survive in mouse bone marrow-derived macrophages (BMDM). Whereas no significant difference was observed at 30 min p.i. (Fig.6A), intramacrophagic survival of Δ*cadC*, Δ*cadAC,* and WT+*lspB* were significantly decreased 5 h p.i., as compared to WT bacteria (Fig.6B). Δ*cadA,* Δ*cadC*+cadC, Δ*lspB* and Δ*cadC*Δ*lspB* behaved similarly to WT. These results indicate that *Lm* phagocytosis is not dependent on CadA, CadC or LspB; high *lspB* expression is detrimental for *Lm* intramacrophagic survival; CadC-mediated repression avoids LspB disruptive effects on *Lm* infection; and the Δ*cadC* phenotype *in vivo* is not related to *cadA* de-repression.

Secreted *Lm* lipoproteins were shown to induce inflammatory cytokines (TNF-α and IL-6) in a TLR2-dependent manner during infection [37]. Given that *lspB* overexpression results in higher LpeA levels in culture supernatants, we tested if this increased lipoprotein release could promote inflammatory cytokine expression. RAW macrophages were infected and 5 h p.i TNF-α and IL-6 expression and secretion levels were assessed. In Δ*lspB*- and Δ*lpeA*-infected RAW, TNF-α and IL-6 levels were significantly reduced. Inversely, infection by *lspB*-overexpressing bacteria resulted in increased cytokine expression/secretion (Fig.6CD). As observed in BMDM, the WT+*lspB* strain showed a significantly reduced capacity to survive in RAW macrophages (Fig.S3B).

Lm thus uses CadC to repress *lspB* expression during infection, avoiding excessive LpeA exposure to the host immune system, reducing inflammatory response and promoting intramacrophagic survival and virulence.

DISCUSSION

CadA is an efflux pump required for Cd resistance, but in contrast to its homologues in *Sa* and *St* [38, 39], it is not essential for zinc and lead efflux and does not significantly contribute to resistance against these or other metals. Whereas *Lm*-CadA was proposed to alternatively transport zinc [40], resistance to zinc was previously shown to

be independent on *Lm*-CadAC [11]. Albeit we cannot exclude that *Lm*-CadA might participate in detoxification of high levels of zinc, it mainly acts as a Cd efflux pump.

Lm-CadC appears as a *trans*-acting, sequence-specific, DNA-binding and Cd-dependent regulator of *cadA, cadC* and *lspB* expression. We show for the first time that the conservation of almost every nucleotide within the Cx palindrome is crucial for CadC binding. As previously suggested [39], we also show that Cd concentration necessary to release CadC from DNA is proportional to the number of Cx. Whereas *cadAC* are generally part of an operon under the control of a unique promoter containing two Cx, in *Lm* these two genes are non-contiguous and controlled by two different Cx-containing promoters. They are separated by *lspB* with the opposite orientation and two Cx between *cadA* and *lspB.* This suggests that *Lm* evolved an additional regulation level allowing a differential regulation of *cadA* and *cadC*. *Lm* appears also as the first bacterium shown to use a Cd efflux pump repressor to control genes unrelated with Cd resistance. This atypical organization of the *cadAC* locus, i.e. split by a SPase-encoding gene, is only found with a remarkable conservation in a cis-mobilisable element of *St* [41]. The chromosomal *Lm-cadAC* locus is predicted as part of a *Lm* integrative and conjugative element [41], and its GC% is markedly lower than that of the surrounding regions, suggesting that *Lm* could have acquired this locus by horizontal gene transfer.

We demonstrate that during infection *Lm* represses *lspB via* CadC to ensure maximal infection efficiency. LspB, as other Gram-positive SPases-II [42], is dispensable for bacterial growth *in vitro* and for virulence *in vivo.* SPases-II specifically process the N-terminal signal peptide of prolipoproteins translocated through the Sec system and lipidated by a diacylglyceryltransferase (Lgt). Lipoproteins are ultimately chained to the membrane *via* a lipid moiety covalently bound to an N-terminal conserved cysteine [43]. In addition to the presence in its sequence of all the conserved domains/residues critical for SPase-II activity [34] and its predicted membrane localization, our results point LspB as a secondary *Lm* SPase-II involved in the processing of LpeA. However, we cannot exclude that LspB could act upon other lipoproteins. LspA, the first SPase-II identified in *Lm,* is involved in lipoprotein processing, including LpeA, and in macrophage phagosome escape [44]. LspA is also involved in lipoprotein release to the extracellular medium, a process also dependent on Lgt. The retention/release of lipoproteins

appears thus as a complex process in *Lm,* co-controlled by Lgt and SPases.

LpeA can be secreted, in particular in absence of Lgt [35, 45]. In a *lgt* mutant, soluble lipoproteins induce the secretion of inflammatory cytokines in a TLR2-dependent manner during infection [37]. *lspB* de-repression/over-expression leads to increased LpeA release and inflammatory cytokines secretion, and correlates with decreased intramacrophage survival and virulence in mice. Interestingly, an *lpeA* mutant survives better inside macrophages and induced early mouse mortality [36]. Group-B *Streptococcus* secreted lipoproteins also activate host inflammatory response through TLR2-signalling [42]. In this model, absence of *lgt* and/or *lsp* leads to decreased TLR2-mediated recognition, reduced inflammatory response, and increased lethality [42]. Secreted mycoplasma lipoproteins also have the ability to modulate the host immune system in a TLR2-dependent manner [46]. Bacteria use thus differently lipoprotein processing enzymes (Lgt, Lsp) to control lipoprotein exposure to host immune recognition mechanisms. While LpeA is required for host cell invasion [36], it also activates host-protective inflammatory responses. To reach a midpoint, *Lm* developed an original strategy to spatially and temporally regulate LpeA exposure at the bacterial surface and to the host immune system. Interestingly, *Lm* downregulates *lgt*, *lspA* and *lspB* and upregulates *cadC* during mouse infection (Tab.S2) [12], suggesting that the localization of *Lm* lipoproteins is tightly regulated during infection to promote virulence.

We propose that *Lm* acquired a mobile element containing the *cadA-lspB-cadC* locus to control lipoprotein localization *via* CadC-dependent *lspB* regulation. During infection, this process minimizes lipoprotein exposure to the host immune system, diminishing inflammatory cytokine expression and promoting intramacrophagic survival and infection. This constitutes the first example of a heavy metal efflux pump regulator repurposed by a bacterial pathogen to fine-tune lipoprotein localization and host immune responses during infection. Being non-essential for bacterial growth, these transcriptional repressors could represent new targets for innovative antibacterial strategies.

Word count: 3 490

ACKNOWLEDGEMENTS

We thank J.H. Morais-Cabral and R. Adaixo (Group of Structural Biochemistry, IBMC) for their help in 3D structure comparison. We thank R. Appelberg for PhD co-supervision of R.P., A.C., O.R., F.C., MT.A. and J.C.P. We thank S. Lamas (Animal Facility), F. Silva (B2Tech), H. Osorio (PCF), P. Magalhães (CCGEN) and R. Fernandes (HEMS) from IBMC facilities for technical assistance.

REFERENCES

1. Saier MH, Jr., Paulsen IT, Sliwinski MK, Pao SS, Skurray RA, Nikaido H. Evolutionary origins of multidrug and drug-specific efflux pumps in bacteria. Faseb J **1998**; 12:265-74.

2. Nies DH. Efflux-mediated heavy metal resistance in prokaryotes. FEMS Microbiol Rev **2003**; 27:313-39.

3. Endo G, Silver S. CadC, the transcriptional regulatory protein of the cadmium resistance system of Staphylococcus aureus plasmid pI258. J Bacteriol **1995**; 177:4437-41.

4. Osman D, Cavet JS. Bacterial metal-sensing proteins exemplified by ArsR-SmtB family repressors. Nat Prod Rep **2010**; 27:668-80.

5. Busenlehner LS, Weng TC, Penner-Hahn JE, Giedroc DP. Elucidation of primary (alpha(3)N) and vestigial (alpha(5)) heavy metal-binding sites in Staphylococcus aureus pI258 CadC: evolutionary implications for metal ion selectivity of ArsR/SmtB metal sensor proteins. J Mol Biol **2002**; 319:685-701.

6. Nucifora G, Chu L, Misra TK, Silver S. Cadmium resistance from Staphylococcus aureus plasmid pI258 cadA gene results from a cadmium-efflux ATPase. Proc Natl Acad Sci U S A **1989**; 86:3544-8.

7. Cossart P. Illuminating the landscape of host-pathogen interactions with the bacterium Listeria monocytogenes. Proc Natl Acad Sci U S A **2011**; 108:19484-91.

8. European Food Safety Authority ECfDPaC. The European Union summary report on trends and sources of zoonoses, zoonotic agents and food-borne outbreaks in 2013. European Food Safety Authority, European Centre for Disease Prevention and Control EFSA Journal **2015**; 13:3991.

9. Swaminathan B, Gerner-Smidt P. The epidemiology of human listeriosis. Microbes Infect **2007**; 9:1236-43.

10. Lebrun M, Audurier A, Cossart P. Plasmid-borne cadmium resistance genes in Listeria monocytogenes are present on Tn5422, a novel transposon closely related to Tn917. J Bacteriol **1994**; 176:3049-61.

11. Lebrun M, Audurier A, Cossart P. Plasmid-borne cadmium resistance genes in Listeria monocytogenes are similar to cadA and cadC of Staphylococcus aureus and are induced by cadmium. J Bacteriol **1994**; 176:3040-8.

12. Camejo A, Buchrieser C, Couve E, et al. In vivo transcriptional profiling of Listeria monocytogenes and mutagenesis identify new virulence factors involved in infection. PLoS Pathog **2009**; 5:e1000449.

13. Glaser P, Frangeul L, Buchrieser C, et al. Comparative genomics of Listeria species. Science **2001**; 294:849-52.

14. Lauer P, Chow MY, Loessner MJ, Portnoy DA, Calendar R. Construction, characterization, and use of two Listeria monocytogenes site-specific phage integration vectors. J Bacteriol **2002**; 184:4177-86.

15. Reis O, Sousa S, Camejo A, et al. LapB, a novel Listeria monocytogenes LPXTG surface adhesin, required for entry into eukaryotic cells and virulence. J Infect Dis **2010**; 202:551-62.

16. Sullivan MA, Yasbin RE, Young FE. New shuttle vectors for Bacillus subtilis and Escherichia coli which allow rapid detection of inserted fragments. Gene **1984**; 29:21-6.

17. Archambaud C, Gouin E, Pizarro-Cerda J, Cossart P, Dussurget O. Translation elongation factor EF-Tu is a target for Stp, a serine-threonine phosphatase involved in virulence of Listeria monocytogenes. Mol Microbiol **2005**; 56:383-96.

18. Leimeister-Wachter M, Domann E, Chakraborty T. The expression of virulence genes in Listeria monocytogenes is thermoregulated. J Bacteriol **1992**; 174:947-52.

19. Kurokawa K, Lee H, Roh KB, et al. The Triacylated ATP Binding Cluster Transporter Substrate-binding Lipoprotein of Staphylococcus aureus Functions as a Native Ligand for Toll-like Receptor 2. J Biol Chem **2009**; 284:8406-11.

20. Pinheiro J, Reis O, Vieira A, et al. Listeria monocytogenes encodes a functional ESX-1 secretion system whose expression is detrimental to in vivo infection. Virulence **2016**:0.

21. Almeida MT, Mesquita FS, Cruz R, et al. Src-dependent tyrosine phosphorylation of non-muscle myosin heavy chain-IIA restricts Listeria monocytogenes cellular infection. J Biol Chem **2015**; 290:8383-95.

22. Lobel L, Sigal N, Borovok I, Belitsky BR, Sonenshein AL, Herskovits AA. The metabolic regulator CodY links Listeria monocytogenes metabolism to virulence by directly activating the virulence regulatory gene prfA. Mol Microbiol **2015**; 95:624-44.

23. Livak KJ, Schmittgen TD. Analysis of relative gene expression data using real-time quantitative PCR and the 2(-Delta Delta C(T)) Method. Methods **2001**; 25:402-8.

24. Cabanes D, Lecuit M, Cossart P. Animal models of Listeria infection. Curr Protoc Microbiol **2008**; Chapter 9:Unit9B 1.

25. Sun Y, Wong MD, Rosen BP. Role of cysteinyl residues in sensing Pb(II), Cd(II), and Zn(II) by the plasmid pI258 CadC repressor. J Biol Chem **2001**; 276:14955-60.

26. Kandegedara A, Thiyagarajan S, Kondapalli KC, Stemmler TL, Rosen BP. Role of bound Zn(II) in the CadC Cd(II)/Pb(II)/Zn(II)-responsive repressor. J Biol Chem **2009**; 284:14958-65.

27. Kuhlbrandt W. Biology, structure and mechanism of P-type ATPases. Nat Rev Mol Cell Biol **2004**; 5:282-95.

28. Kuenne C, Voget S, Pischimarov J, et al. Comparative analysis of plasmids in the genus Listeria. PLoS One **2010**; 5.

29. Bierne H, Cossart P. Listeria monocytogenes surface proteins: from genome predictions to function. Microbiol Mol Biol Rev **2007**; 71:377-97.

30. Desvaux M, Hebraud M. The protein secretion systems in Listeria: inside out bacterial virulence. FEMS Microbiol Rev **2006**; 30:774-805.

31. Milohanic E, Glaser P, Coppee JY, et al. Transcriptome analysis of Listeria monocytogenes identifies three groups of genes differently regulated by PrfA. Mol Microbiol **2003**; 47:1613-25.

32. Scortti M, Monzo HJ, Lacharme-Lora L, Lewis DA, Vazquez-Boland JA. The PrfA virulence regulon. Microbes Infect **2007**; 9:1196-207.

33. Stoll R, Mertins S, Joseph B, Muller-Altrock S, Goebel W. Modulation of PrfA activity in Listeria monocytogenes upon growth in different culture media. Microbiology **2008**; 154:3856-76.

34. Tjalsma H, Zanen G, Venema G, Bron S, van Dijl JM. The potential active site of the lipoprotein-specific (type II) signal peptidase of Bacillus subtilis. J Biol Chem **1999**; 274:28191-7.

35. Baumgartner M, Karst U, Gerstel B, Loessner M, Wehland J, Jansch L. Inactivation of Lgt allows systematic characterization of lipoproteins from Listeria monocytogenes. J Bacteriol **2007**; 189:313-24.

36. Reglier-Poupet H, Pellegrini E, Charbit A, Berche P. Identification of LpeA, a PsaA-like membrane protein that promotes cell entry by Listeria monocytogenes. Infect Immun **2003**; 71:474-82.

412 37. Machata S, Tchatalbachev S, Mohamed W, Jansch L, Hain T, Chakraborty T. Lipoproteins of Listeria
413 monocytogenes are critical for virulence and TLR2-mediated immune activation. J Immunol **2008**; 181:2028-35.
414 38. Yoon KP, Silver S. A second gene in the Staphylococcus aureus cadA cadmium resistance determinant of
415 plasmid pI258. J Bacteriol **1991**; 173:7636-42.
416 39. Schirawski J, Hagens W, Fitzgerald GF, Van Sinderen D. Molecular characterization of cadmium resistance in
417 Streptococcus thermophilus strain 4134: an example of lateral gene transfer. Appl Environ Microbiol **2002**;
418 68:5508-16.
419 40. Banci L, Bertini I, Ciofi-Baffoni S, et al. Structural basis for metal binding specificity: the N-terminal cadmium
420 binding domain of the P1-type ATPase CadA. J Mol Biol **2006**; 356:638-50.
421 41. Pavlovic G, Burrus V, Gintz B, Decaris B, Guedon G. Evolution of genomic islands by deletion and tandem
422 accretion by site-specific recombination: ICESt1-related elements from Streptococcus thermophilus. Microbiology
423 **2004**; 150:759-74.
424 42. Henneke P, Dramsi S, Mancuso G, et al. Lipoproteins are critical TLR2 activating toxins in group B
425 streptococcal sepsis. J Immunol **2008**; 180:6149-58.
426 43. Sankaran K, Wu HC. Lipid modification of bacterial prolipoprotein. Transfer of diacylglyceryl moiety from
427 phosphatidylglycerol. J Biol Chem **1994**; 269:19701-6.
428 44. Reglier-Poupet H, Frehel C, Dubail I, et al. Maturation of lipoproteins by type II signal peptidase is required for
429 phagosomal escape of Listeria monocytogenes. J Biol Chem **2003**; 278:49469-77.
430 45. Trost M, Wehmhoner D, Karst U, Dieterich G, Wehland J, Jansch L. Comparative proteome analysis of
431 secretory proteins from pathogenic and nonpathogenic Listeria species. Proteomics **2005**; 5:1544-57.
432 46. Seya T, Matsumoto M. A lipoprotein family from Mycoplasma fermentans confers host immune activation
433 through Toll-like receptor 2. Int J Biochem Cell Biol **2002**; 34:901-6.
434 47. Dramsi S, Kocks C, Forestier C, Cossart P. Internalin-mediated invasion of epithelial cells by Listeria
435 monocytogenes is regulated by the bacterial growth state, temperature and the pleiotropic activator prfA. Mol
436 Microbiol **1993**; 9:931-41.

48. Claros MG, von Heijne G. TopPred II: an improved software for membrane protein structure predictions. Comput Appl Biosci **1994**; 10:685-6.

FIGURE LEGENDS

Figure 1. Identification of a cadmium resistance system in the genome of *Lm*

(A) Alignment of the CadC and CadA protein sequences of *Lm* and *Sa* pI258. Metal-binding sites 1 (red boxes) and 2 (blue boxes) are indicated. Green box indicates CXXC metal-binding site. Yellow box shows CPC motif and orange box indicates DKTGTLT sequence. (B) *Lm* genomic organization and GC content of the region encompassing *cadAC*. Variations in the DNA GC% relative to the average GC% of the whole genome are indicated by bars. Numbers correspond to the GC% for each gene. (C) Transcriptional analysis of the *cadA-lspB-cadC* region by RT-PCR. Predicted fragments (*cadA*, *cadA-lspB*, *lspB*, *lspB-cadC* and *cadC*) amplified with the different primer sets are indicated on the schematic representation of the *cadA-lspB-cadC* locus. RT-PCRs were performed on RNAs from logarithmic cultures of *Lm* growing in BHI broth at 37ºC, in the absence (-) or presence (+) of cadmium (Cd). Control PCRs were performed on genomic DNA. (D) Analysis of PrfA regulation of *cadC* transcription. Quantitative real-time PCR was performed on RNAs extracted from logarithmic cultures of WT and Δ*prfA* strains grown in BHI at 37°C. *inlA* and *lmo2845* were used as PrfA-dependent and PrfA-independent control genes, respectively [47] [15]. Gene expression levels in the Δ*prfA* mutant are presented normalized to those in the WT (set at 1). Values are mean ± SD from 3 independent experiments. Statistical significance is indicated as compared to WT: **P*<0.05

Figure 2. CadA behaves as a cadmium efflux pump required for *Lm* resistance to cadmium

(A) Growth curves of the WT, Δ*cadA*, Δ*cadC* and Δ*cadAC* strains in BHI at 37°C and challenged at t=210 min with 384 μM $CdCl_2$. Representative results from three independent experiments. (B) Growth inhibition of WT,

462 Δ*cadA* and Δ*cadC* strains in agar medium overlaid with disks saturated with 100 mM $CdCl_2$ or $CdSO_4$, or with 100
463 mM of zinc (Zn), lead (Pb), manganese (Mn), cobalt (Co), copper (Cu), calcium (Ca), magnesium (Mg) or nickel
464 (Ni) salts. Values are mean ± SD from 5 independent experiments. (C) MICs of cadmium, zinc, cobalt, copper and
465 nickel for the WT and Δ*cadA* strains. (D) Intracellular levels of cadmium, zinc and lead measured by ICP-MS in the
466 WT and Δ*cadA* strains. Values are mean ± SD from 3 independent experiments. **P*<0.05 and ****P*<0.001.
467
468 **Figure 3. CadC directly regulates *cadA, cadC* and *lspB* expression in response to cadmium**
469 (A) *cadA, cadC* and *lspB* transcription is dependent on CadC and Cd concentration. qRT-PCRs on RNAs
470 extracted from logarithmic cultures of WT and Δ*cadC* grown in BHI at 37ºC and WT grown in BHI supplemented
471 with Cd (WT+Cd). *lmo2845* was used as a CadC- and Cd-independent control gene. Gene expression levels are
472 shown normalized to those in the WT grown in BHI in absence of Cd (set at 1). Values are mean ± SD from 3
473 independent experiments. Statistical significance is indicated as compared to WT: **P*<0.05 and ***P*<0.01. (B)
474 CadC binds directly *cadA*, *cadC* and *lspB* CadC box. (Upper panel) Alignment of CadC boxes upstream of *Sa*
475 pI258 *cadC* (*SacadC*), *Lm cadA* (*LmcadA*), *Lm cadC* (*LmcadC*) and *Lm lspB* (*LmlspB*). Palindromes are indicated
476 by arrows. (Bottom left panel) Increasing amounts of purified CadC were used in electrophoretic mobility shift
477 assays (EMSAs) with DNA fragments containing the *cadA*, *cadC* or *lspB* CadC box (Cx) generated by PCR using
478 primers listed in Table S1. An unrelated promoter region (*inlA*) and an unrelated protein (GFP) were used as
479 negative controls. (Bottom right panel) ChIP-qPCR was conducted to quantify the capacity of CadC to bind Cx *in*
480 *vivo*. Fold enrichment is shown normalized to an unrelated promoter region (*inlA*) and as compared to mock-IP.
481 Values are mean ± SD from 5 independent experiments. **P*<0.05. (C) Specificity of the CadC-Cx interaction using
482 Cx-containing DNA fragments in which the palindromic sequence was either present in its unaltered form (Cx), or
483 containing point (Cx-M1-5), or transversed (Cx-T) mutations (indicated in red). (D) In the presence of Cd, CadC
484 fails to bind *cadA, cadC* and *lspB* Cx. Increasing amounts of $CdCl_2$ were used in EMSAs with purified CadC and
485 *cadA* Cx, *cadA* Cx-*lspB* Cx and *cadC* Cx DNA fragments. (B-D) Experiments were performed at least twice, and
486 representative results are shown.

Figure 4. In absence of CadC repression, *lspB* expression is deleterious for *Lm* infectious capacity

(A) Bacterial counts of the WT, Δ*cadA*, Δ*cadC,* Δ*cadAC* and Δ*cadC*+*cadC* strains in the liver and spleen of C57BL/6 mice 72h after intravenous inoculation of 10^5 bacteria per animal. (B) Bacterial counts of the WT, Δ*cadA*, Δ*cadC* and Δ*cadAC* strains in the liver and spleen of C57BL/6 mice 72h after oral inoculation of 10^9 bacteria per animal. (C) Bacterial counts of the WT, Δ*lspB*, Δ*cadC*Δ*lspB* and WT+*lspB* strains in the liver and spleen of C57BL/6 mice 72h after intravenous inoculation of 10^5 bacteria per animal. (D) Bacterial counts of the WT, Δ*lspB*, Δ*cadC*Δ*lspB* and WT+*lspB* strains in the liver and spleen of BALB/c mice 72h after oral inoculation of 10^9 bacteria per animal. Data are presented as scatter plots, with each animal indicated by empty circle and the mean indicated by a horizontal line. (n=5). **P*<0.05, ***P*<0.01 and ****P*<0.001.

Figure 5. LspB controls LpeA release in the extracellular medium

(A) Alignment of the protein sequence of SPases II from *Lm* (*Lm* LspA and *Lm* LspB), *Listeria innocua* (*Lin* Lsp), *Bacillus subtilis* (*Bs* Lsp), *Sa* (*Sa* Lsp) and *St* (*St* Lsp). Residues present in at least 3 SPases II are in blue while residues conserved in all SPases II are shown in red. Conserved domains (I-V) as defined by Tjalsma *et al.* [34], are highlighted in green boxes. Residues important for activity/stability are indicated by green arrows. (B) Lipoprotein membrane extracts and culture supernatants from the WT, Δ*cadC*, Δ*lspB,* Δ*cadC*Δ*lspB* and WT+*lspB* strains separated by SDS-PAGE and stained with Coomassie Blue. Arrows indicate a band between 25 and 37 kDa with increased intensity in the culture supernatants from Δ*cadC* and WT+*lspB* strains. (C) Quantifications of LpeA in culture supernatants (ImageJ). Values are mean ± SD from 3 independent experiments and are presented normalized to loading control and as percentage relative to the mean of WT band intensity (set at 100). **P*<0.05 and ***P*<0.01.

Figure 6. In absence of CadC repression, *lspB* expression decreases *Lm* survival in macrophages and induces inflammatory cytokine expression

(A-B) Intracellular numbers of the WT, Δ*cadA*, Δ*cadC,* Δ*cadC*+*cadC,* Δ*cadAC,* Δ*lspB,* WT+*lspB* and Δ*cadC*Δ*lspB* strains in mouse bone marrow-derived macrophages (BMDM) at (A) 30 min and (B) 5 h post-infection (p.i.). Values are mean ± SD from 3 independent experiments and are presented as percentage relative to the mean of WT bacterial counts (set at 100). Statistical significance is indicated as compared to WT: **P*<0.05, ***P*<0.01 and ****P*<0.001, or between indicated strains: ###*P*<0.001. (C-D) Quantification of TNF-α and IL-6 expression levels by qRT-PCR (C) and secretion levels by ELISA (D) at 5 h p.i. of RAW macrophages with either WT*,* Δ*lspB,* WT+*lspB* or Δ*lpeA* strains. Values are mean ± SD from 3 independent experiments. Statistical significance is indicated as compared to WT: **P*<0.05, ***P*<0.01 and ****P*<0.001.

Figure S1. (A) Amino acid identity between CadC and CadA proteins from *Lm* and other bacteria. (B) Comparison of the 3D structure of *Sa* pI258 CadC dimer (blue and green) and the predicted 3D structure of *Lm* CadC dimer (red). The *Lm*-CadC structure was predicted using I-TASSER and matched to the solved structure of *Sa* pI258 CadC with PyMOL software. (C) Membrane topology model of *Lm* CadA as predicted by TopPred II software [48]. (D) Model for the membrane topology of LspB. The orientation of putative transmembrane regions was predicted with the TopPred II software [48]. Conserved domains I-V are indicated.

Figure S2. (A) Purification of recombinant CadC protein. SDS-PAGE analysis of Ni-NTA agarose column chromatography of CadC-His_6 protein after Coomassie blue staining. (B). Growth curves of the WT, Δ*cadA*, Δ*lspB* and Δ*cadC*Δ*lspB* strains in BHI at 37°C and challenged at t=210 min with 384 μM $CdCl_2$. (C) Growth curves of the WT, Δ*cadA*, Δ*cadC,* and Δ*cadC*+*cadC* strains in BHI at 37°C. (D) Growth curves of the WT, Δ*lspB*, Δ*cadC*Δ*lspB* and WT+*lspB* strains in BHI at 37°C. (E) RT-PCR analysis of the *lspB* expression in WT and WT+*lspB* strains. (F) Transmission electron microscopy analysis of the WT, Δ*cadC* and WT+*lspB* bacteria. Scale bar: 0.2 μm.

Figure S3. (A) Analysis of *lspA* expression. Quantitative real-time PCR was performed on RNAs extracted from logarithmic cultures of WT, Δ*cadC*, Δ*lspB,* Δ*cadC*Δ*lspB* and WT+*lspB* strains grown in BHI at 37°C. Gene

expression levels are presented normalized to those in the WT (set at 1). Values are mean ± SD from 3 independent experiments. (B) Intracellular multiplication of the WT and WT+*lspB* strains in RAW macrophages at 5 h p.i. Values are mean ± SD from 3 independent experiments and are presented as percentage relative to the mean of WT bacterial counts (set at 100). Statistical significance is indicated as compared to WT: ** $P<0.01$.

Table S1 - Primers

Primer name	Sequence (5' to 3')
Primers used for mutagenesis	
lmo1100MA	ATAGTCGACAGTAGCGACTACTTCACACC
lmo1100MB	CGACGCGTCATAAAATTCCTCCTTTTTC
lmo1100MC	CGACGCGTCTAATGAAACTTACAAGG
lmo1100MD	CGCAGATCTAACTTTGTTTCTAACATTCG
lmo1101MA	ATAGTCGACCAACATCATCACGACGTA
lmo1101MB	CGAATTCCATATCAACTCACTTGGAG
lmo1101MC	CGAATTCTAGCCTTTTTTCAAGTAGAAG
lmo1101MD	CAACCATGGGTGACGGAACTGTGGACGCA
lmo1102MA	CGAGTCGACTTCCCACTATCAAAGTGG
lmo1102MB	CGAATTCCACGTTCCTAAACACTCC
lmo1102MC	CGAATTCTAAAAAAATCTTCAAACAC
lmo1102MD	CGCAGATCTAATTCGTACAAGACATACC
lpeAMA	AGAGCTCGGGTGTTCCAGTCAAAATAGC
lpeAMD	ACAGTCGACGCCTTTTTTGCAGTGGAGTC
Primers used for complementation	
lmo1102CG	GCCACTAGTAACCCTGTTTACACACAAGC
lmo1102CH	ACCGTCGACTAGTCCGTGACTCTTTAGAC
Primers used for overexpression	
lmo1101OA	GACGGATCCGAGTTGATATGAAAAATAAGAC
lmo1101OB	CAGCTGCAGGCTACATTTTTTTGTAACTAAC
Primers used for cloning in pET28b	
lmo1102P1	TACCATGGTGAATGACATTTGTGAAATAAC
lmo1102P2	ACTCGAGAAGTACAATATCTTTGATTAATG
Primers used for qRT-PCR	
16SqF	CTCGTGTCGTGAGATGTTGG
16SqR	CGTGTGTAGCCCAGGTCATA
inlAqF	ACAACTGGAGGGAACGCGCC
inlAqR	CCAGGTATATTTGCGGAAGG
lmo1100qF	TGAACGAGCACCAGCACAAGCG
lmo1100qR	CCCATGTGTCCCAATCACCACC
lmo1101qF	TCAAGATAACATACGCTCAA
lmo1101qR	CCATTAACGCTACTCCAA
lmo1102qF	AAGCCCTATCTGAAGAAACTAGG
lmo1102aR	CGCTACTGTTGATTTCACAATG
lmo2845qF	GGTGTAGGAACTGCCATCGGACC
lmo2845qR	ACTGCGCGCCAACCATTTGTAGC
hprt1qF	TGATTAGCGATGATGAACCA
hprt1qR	GTCTTTCAGTCCTGTCCATAA
TNFαqF	CCAAAGGGATGAGAAGTTC
TNFαqR	GAGAAGATGATCTGAGTGTG
IL-6qF	GACCTGTCTATACCACTTCAC
IL-6qR	GCCATTGCACAACTCTTTTC
lspApF	TTATTCTAGGTGGTGCGATTGG
lspAqR	TTCGTTTTGCGGTCGTCTAC

Primers used for EMSA	
inlAEF	GGCTCCGTAGACAGATTAGC
inlAER	ACTTTTCAACCATACATATCG
lmo1100EF	CATTTACTTACCTTAAGACAAG
lmo1100ER	CGTACAAGACATACCGTCTAC
lmo1101EF	ATAATCTGATATTATGTATTTG
lmo1101ER	CAAATACATAATATCAGATTAT
lmo1102EF	AGCTTTCTTCTTTTGCTCGC
lmo1102ER	GAACCTTTTCCTCATCAAAAC
Primers used for ChIP-qPCR	
cadCChIPF	TCCTAAACACTCCTTTTCAA
cadCChIPR	TCTTTTGCTCGCATAATAGT
cadAChIPF	GCACAATTCGTACAAGAC
cadAChIPR	TCAAACAAACACTTGAATGT
lspBChIPF	CATTCAAGCGTTTGTTTG
lspBChIPR	CTTCATTTAACGTCTCCTTT
inlABChIPF	CAATTCGTGGGGAGCATA
inlABChIPR	TCAGGTTTCGTTGTATAGGA

Table S2 – *Lm* gene expression fold change during mouse infection

Gene name	Gene code	Fold change (spleen/BHI 37ºC)*
lspB	*lmo1101*	**-3,3**
cadC	*lmo1102*	**9,7**
lspA	*lmo1844*	**-3,3**
lgt	*lmo2482*	**-2,3**

* Data from Camejo *et al*, PLoS Pathog. 2009; 5(5):e1000449

Table S3

Protein name: LpeA (310 aa) ***lmo*:** *lmo1847* **Mass:** 34453 **Score:** 116 **Expect:** 7.2×10^{-9} **Matches:** 29

Peptide	Position
KTDGKLNVVATYSILADIVK	28 - 47
TDGKLNVVATYSILADIVK	29 - 47
LNVVATYSILADIVK	33 - 47
YLTEKGK	127 - 133
YLTEKGKTSETDPHAWLDLHNGIIYTENVR	127 - 156
GKTSETDPHAWLDLHNGIIYTENVR	132 - 156
GKTSETDPHAWLDLHNGIIYTENVRDALVK	132 - 161
TSETDPHAWLDLHNGIIYTENVR	134 - 156

TSETDPHAWLDLHNGIIYTENVRDALVK	134 - 161
YIDKLATLDKEAK	177 - 189
QKFADLPENQK	190 - 200
FADLPENQK	192 - 200
FADLPENQKTLVTSEGAFK	192 - 210
FADLPENQKTLVTSEGAFKYFAAR	192 - 215
TLVTSEGAFKYFAAR	201 - 215
AAYIWEINTESQGTPDQMK	220 - 238
AAYIWEINTESQGTPDQMKQIVGIVEKEK	220 - 248
QIVGIVEKEKVPNLFVETSVDPR	239 - 261
EKVPNLFVETSVDPR	247 - 261
VPNLFVETSVDPR	249 - 261
SMESVSKETGVPIFAK	262 - 277
SMESVSKETGVPIFAK	262 - 277
ETGVPIFAK	269 - 277
IFTDSTAK	278 - 285
IFTDSTAKKGEVGDTYLEMMR	278 - 298
IFTDSTAKKGEVGDTYLEMMR	278 - 298
KGEVGDTYLEMMR	286 - 298
GEVGDTYLEMMR	287 - 298
YNLDKIHDGLAK	299 - 310

Coverage: 185/310 aa = 59,7 %

MKKIIVVSLFALVVVLAGCSSQNSDSKK**TDGKLNVVATYSILADIVK**NVGGNKIELHSIVPVGVDPHEYDPLPANIQSAADADLIFYN
TADKSREDKNQVVELSKGVKPK**YLTEKGKTSETDPHAWLDLHNGIIYTENVRDALVK**ADPDNADFYKENAKK**YIDKLATLDKEA**
GAFKYFAARYGLK**AAYIWEINTESQGTPDQMKQIVGIVEKEKVPNLFVETSVDPRSMESVSKETGVPIFAKIFTDSTAKKGEVGD**

548

Figure 1

Click here to download Figure Pombinho-JID-Figures-Rev_1.eps

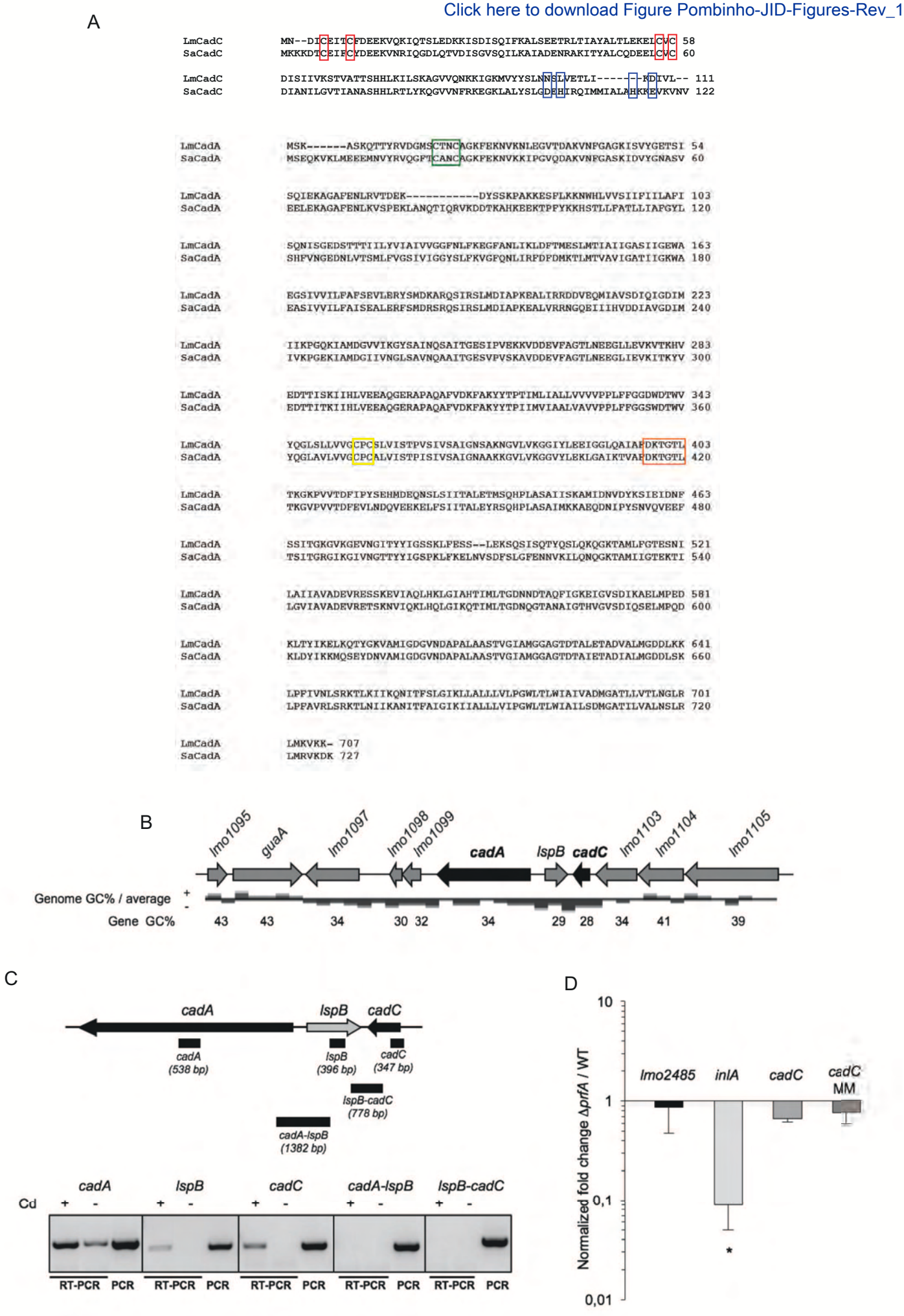

Figure 1

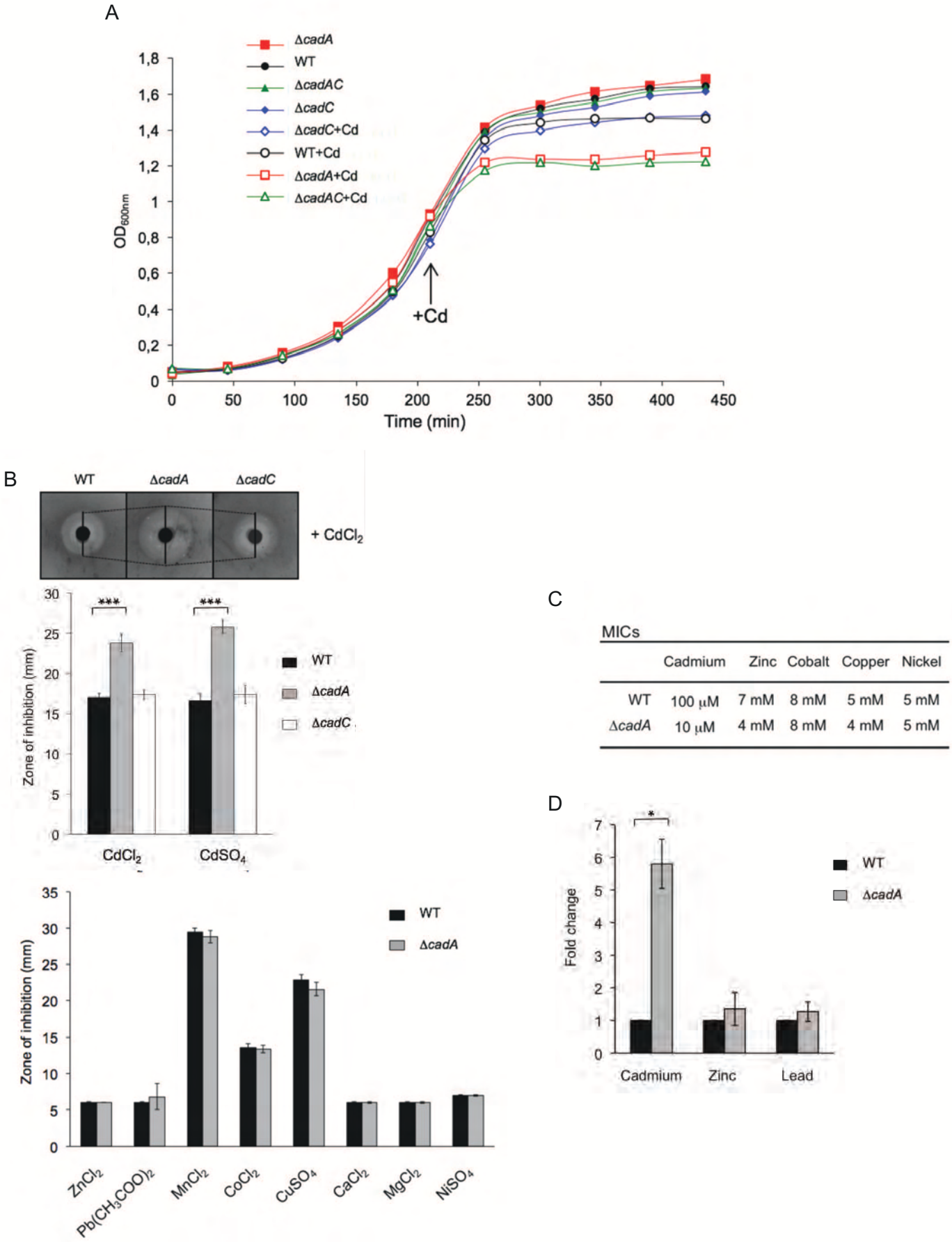

Figure 2

Figure 3

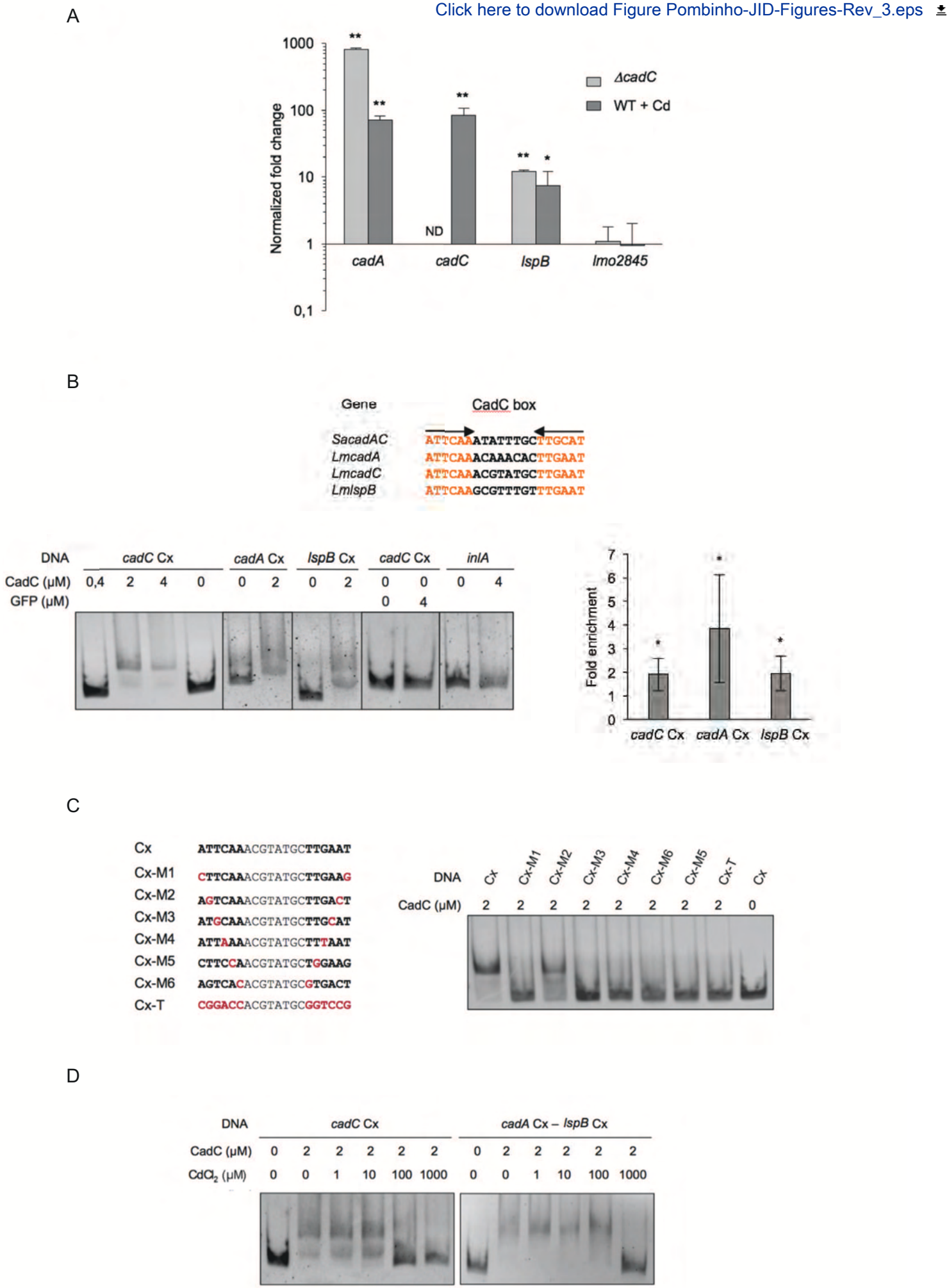

Figure 3

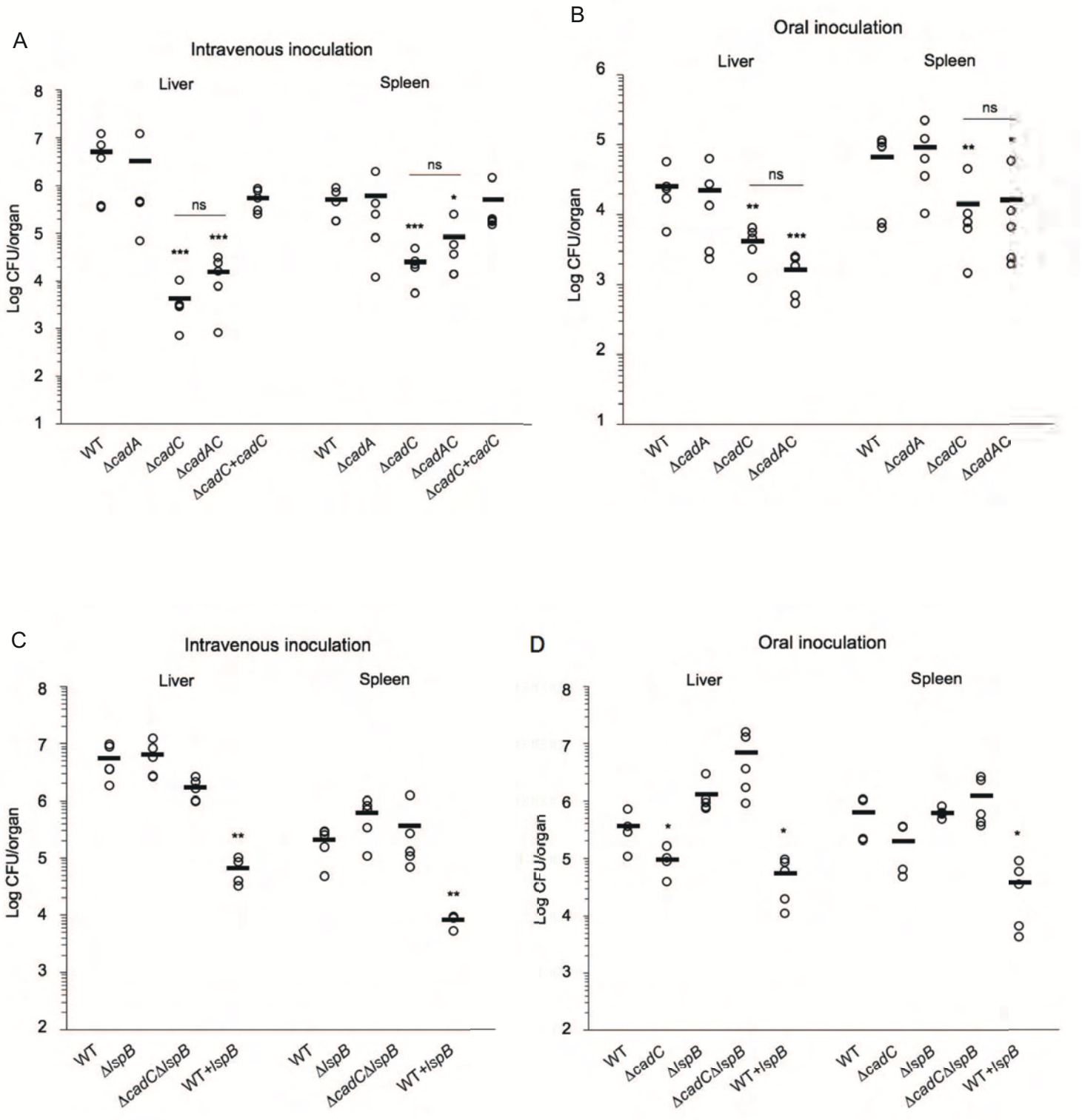

Figure 4

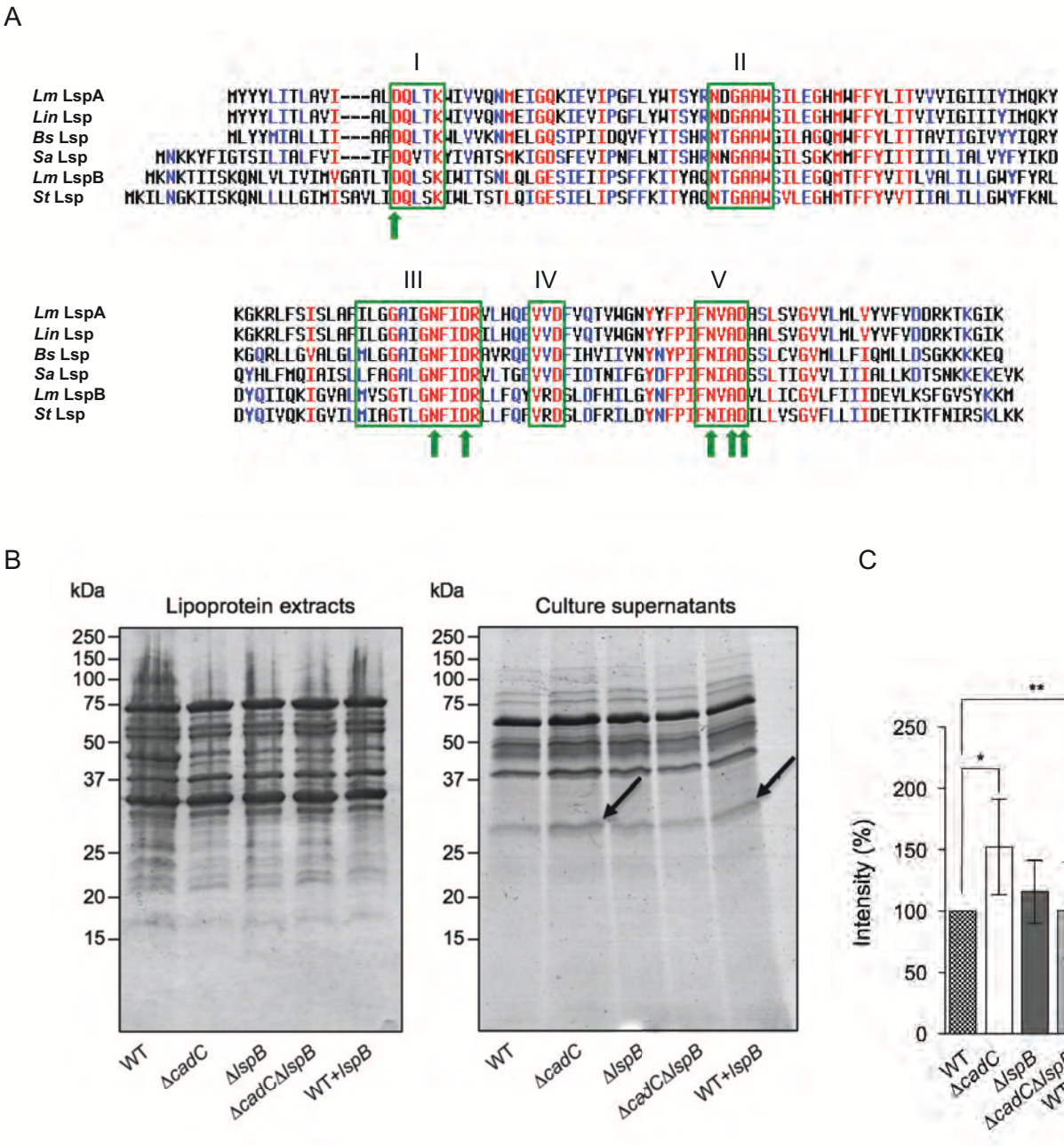

Figure 5

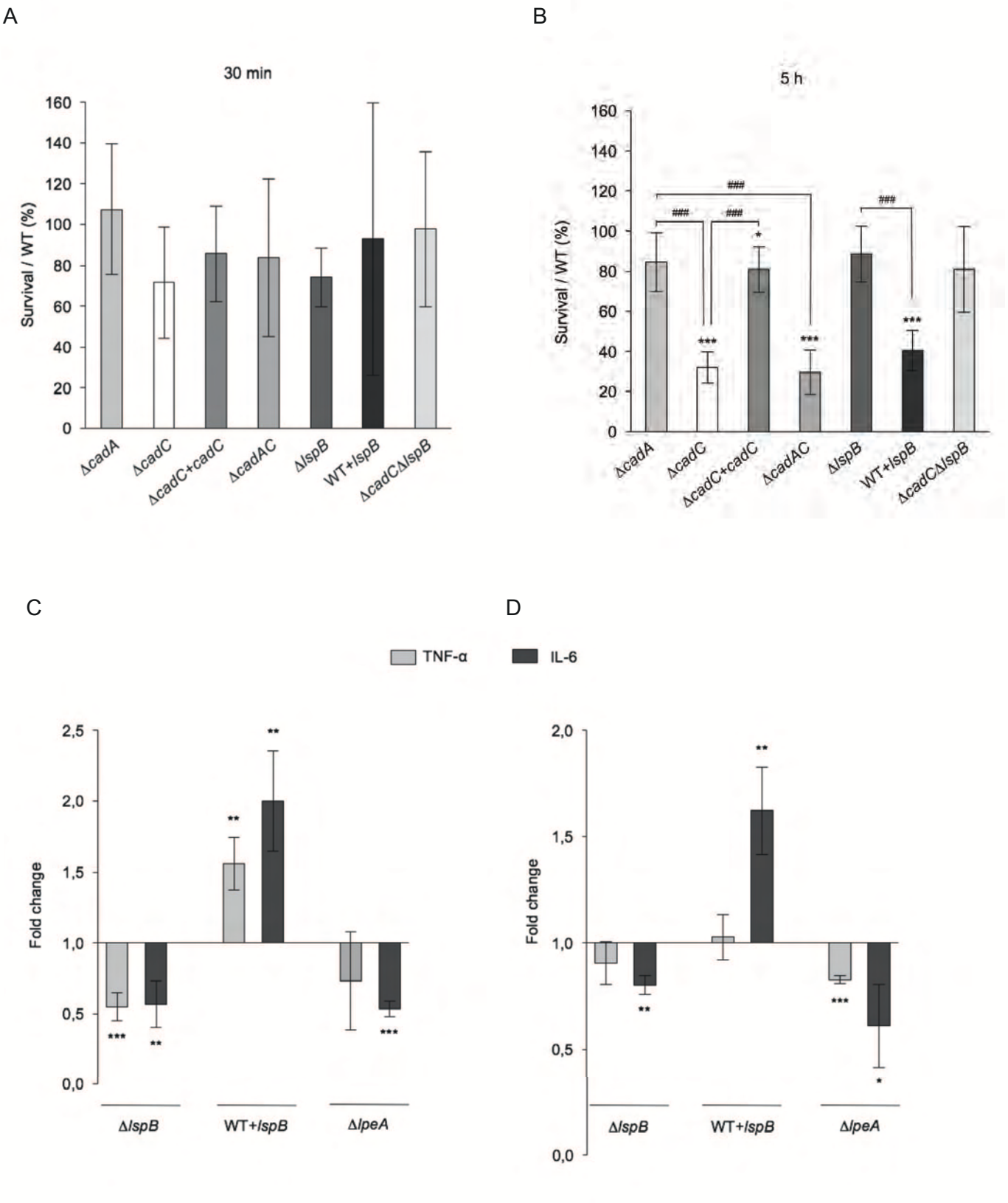

Figure 6

Figure S1

Click here to download Figure Pombinho-JID-Figures-Rev_S1.eps

A

Amino acid identity between CadC and CadA proteins from several organisms

Species	Strain	Location	Identity with CadC/CadA
S. aureus	RN4220	Plasmid pI258	48%/67%
S. thermophilus	4134	Chromosome	90%/95%
L. monocytogenes	Lm74	Plasmid Lm74	58%/70%
L. innocua	CLIP 11262	Plasmid	52%/73%

B

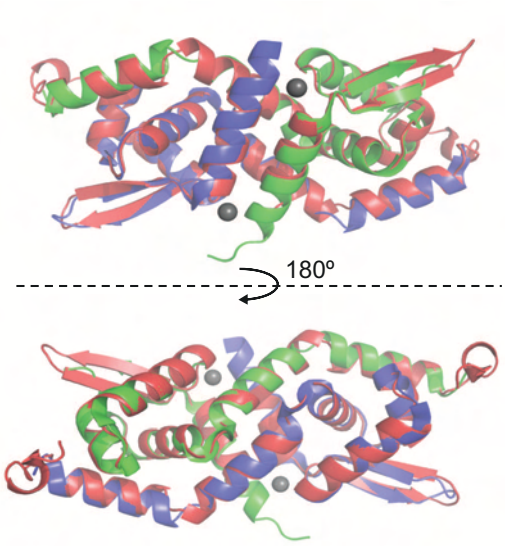

C

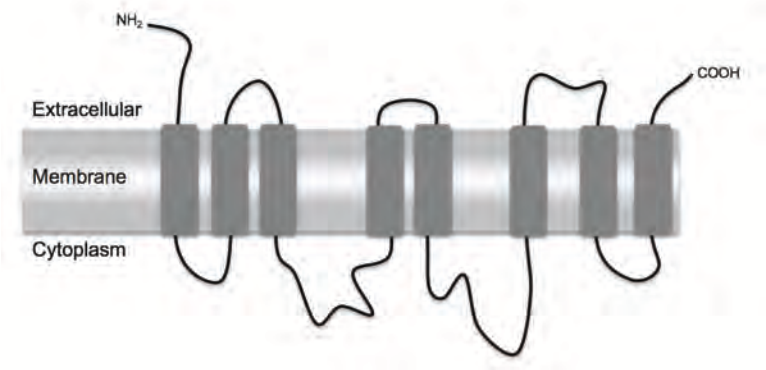

D

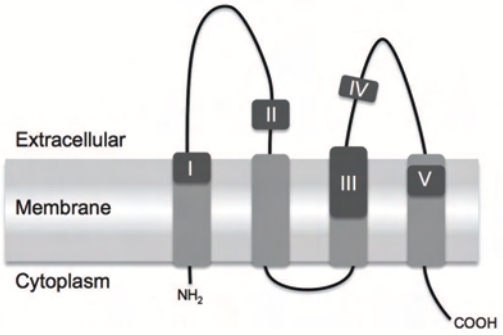

Figure S1

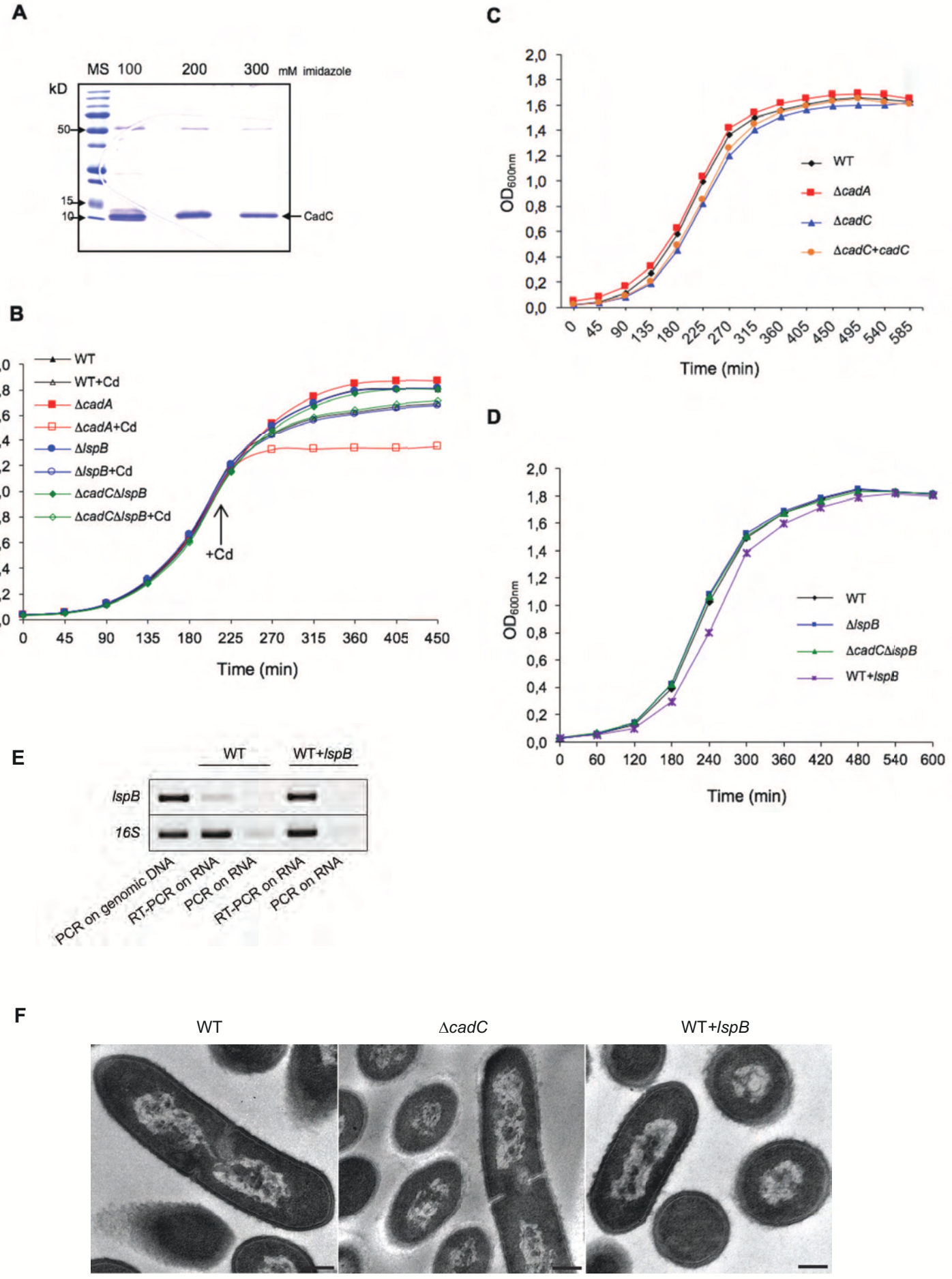

Figure S2

Figure S3

Click here to download Figure Pombinho-JID-Figures-Rev_S3.eps

A

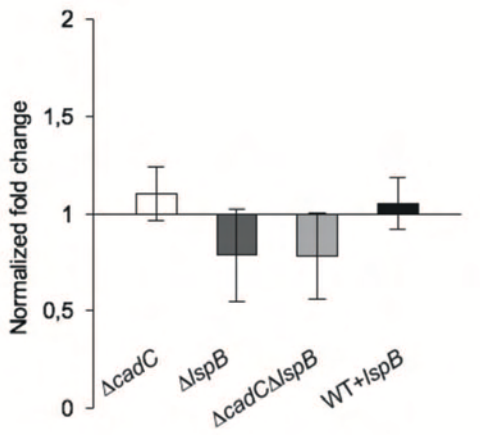

B

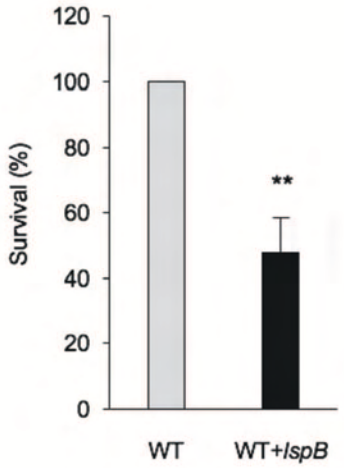

Figure S3